Advances in Science and Technology Research Journal

Advances in Science and Technology Research Journal 2022, 16(6), 275–285
https://doi.org/10.12913/22998624/156412
ISSN 2299-8624, License CC-BY 4.0

Received: 2022.10.31
Accepted: 2022.11.18
Published: 2022.12.01

Evaluation of Wind Energy Potential in View of the Wind Speed Parameters – A Case Study for the Southern Jordan

Sameh Alsaqoor[1,2*], Abdullah Marashli[3], Reem At-Tawarah[3], Gabriel Borowski[4], Ali Alahmer[2,5], Nader Aljabarin[6], Nabil Beithou[2]

[1] Renewable Energy Technology, Department of Engineering and Technology, Applied Science Private University, P.O. Box 166, Amman, 11931 Jordan

[2] Department of Mechanical Engineering, Faculty of Engineering, Tafila Technical University, P.O. Box 179, 66110 Tafila, Jordan

[3] Mechanical Engineering Department, Faculty of Engineering, Al-Hussein Bin Talal University, Ma'an 71111, Jordan

[4] Faculty of Environmental Engineering, Lublin University of Technology, ul. Nadbystrzycka 40B, 20-618 Lublin, Poland

[5] Department of Industrial and Systems Engineering, Auburn University, Auburn, AL 36849, USA

[6] Natural Resources and Chemical Engineering Department, Faculty of Engineering, Tafila Technical University, P.O. Box 179, 66110 Tafila, Jordan

* Corresponding author's email: s_alsqoor@asu.edu.jo

ABSTRACT

In this paper, the potential resources of wind energy were examined, in the case of three different locations in Southern Jordan. On the basis of the collection of wind speed data, this study attempted to estimate the potential wind power. The empirical analysis was conducted using three different numerical approaches: empirical method, energy pattern factor method, and method of the moment. Afterward, the energy yield was evaluated including Weibull parameters, such as shape parameter and scale parameter. The analysis findings helped designate the most prospective locations for developing the strong wind energy potential. The annual mean values of wind speed observed in the typed locations were from 3.9 m/s to 4.9 m/s, and the theoretical wind power density distributions were from 87.6 W/m^2 to 126.8 W/m^2. The Aqaba area would be the most promising wind power location due to the greatest wind energy potential.

Keywords: wind energy potential, wind speed, wind turbine, Weibull distribution.

INTRODUCTION

The increased growth rate of electricity demand, which is linked to an increase in the cost of energy production, surpasses the energy sector's intentions to develop a strategy for maximizing the efficiency of existing production sources [1–4]. Jordan is taking the steps to improve and diversify its electrical system, with natural gas accounting for 87% of electricity generation in conventional power plants and renewable energy accounting for 13% at the end of 2019, up from 11% renewable energy and 89% natural gas in 2018 [5–7]. Wind energy is one of the prospective options for energy sector development on a large scale. The location chosen for a wind farm installation is critical to the project's success. The following are the most significant aspects and criteria for the construction of wind farms and the selection of a wind project site [8, 9]: (i) land with a good wind resource, (ii) installable windy area, (iii) grid connection and access to transmission lines and carrying capacity, (iv) transportation to transport all wind types of equipment from

monitoring and building to the location, (v) land use off-limits such as military use, wildlife sanctuary, historical or religious, and (vi) residential areas. There are also additional issues to consider, including the agreement to sell energy generated, the land leasing agreement with the landowner, as well as the communications and cellular data transmission availability.

Many statistical models have been developed and examined for various locations in order to estimate the potential of wind energy. These models assist energy planners, researchers, and policymakers in various ways. Wind power is a function of wind speed; the approach is based on the constructing of a model for estimating values of wind power by applying appropriate transformations to wind speed measurements [10]. Chang [11] used several approaches to derive the Weibull parameters to evaluate the wind power density from wind speed data for four sites. The results showed that the graphical method (GM) yielded results for all four stations. Still, energy pattern factor method (EPFM) was the most suited for the two sites, and empirical method (EM) displayed the greatest outcomes for the other two stations. Ouahabi et al. [12] conducted a statistical analysis regarding of the different methods of Weibull distribution functions to predict the wind potential in the Tetouan area of Northern Morocco. Except for the graphical method, the findings reveal that the method of moment (MOM), EPFM and EM offered more accurate results and are quite comparable to the predictions made by the different Weibull curves. Azad et al. [13] compared seven Weibull estimating techniques to estimate wind potential. According to the study, the MOM and maximum likelihood method (MLM) are the best strategies at any height. In India, Ramachandra et al. [14] investigated the wind potential in Kumta and Sirsi by collecting primary data from the Indian meteorological department. The results showed that the EPFM is a more suitable approximation of the Weibull probability density function (PDF) for the wind speed.

The wind potential in Jeddah, Saudi Arabia, was investigated using wind meteorological data obtained at the height of 10 meters with GM and MOM by Bassyouni et al. [15]. The location was considered a promising option for small-scale off-grid wind energy use. Aukitino et al. [16] compared seven approaches for assessing wind resources at two locations in Kiribati. The findings revealed that the (MOM) method was the best overall and was then used to assess power density. Kidmo et al. [17] used six numerical approaches to determine the Weibull parameters to simulate the wind speed distribution in Garoua, Cameroon. The EPFM performed the best, according to the results. Marashli et al. [18] arrived at the same conclusions as the previous research. The EPFM methodology, according to the author, is the most accurate and efficient method for calculating the Weibull distribution parameters. Alsaad [19] used the data from the local meteorological agency to investigate the potential of wind energy in many Jordanian sites (Ras Moneef, Al-Fjaij, Al-Hasan, and Al-Safawi). The findings encouraged the construction of potential 100 MW wind turbines for energy generation in a few Jordanian locations. Bataineh and Dalalah [20] introduced a technical assessment of wind power potential for seven places in Jordan (Hofa, Ibrahimya, Ras Monief, Tafila, Zabda, Fujaij, and Aqaba) based on the recorded wind data using statistical analysis. To model the monthly average data and estimate the wind power in the specified sites, the Rayleigh distribution was utilized. With wind turbines of various sizes, energy estimates, capacity factors, and cost of wind energy generation were computed for the specified locations. Jordan's high potential for wind energy has been proven, and the development of wind energy can assist Jordan in meeting its environmental and energy policy goals. Ammari et al. [21] studied and evaluated the wind power for five distinct sites in Jordan (Ras-Moneef, Azraq South, Safawi, Queen Alia Airport, and Aqaba Airport) using the data from mean monthly wind speeds during a typical year. In addition, the feasibility of employing five distinct wind turbines at each location for use in wind farms was investigated.

The EM technique was also used to compute the value of the Weibull parameters. The authors concluded that the wind speed data over the last five years is fitted to the Weibull distribution, which is the most often used and suited for characterizing the frequency distribution of wind flowing across Jordan. The greatest values of k and c parameters may be found at Aqaba Airport. Alrwashdeh [22] employed mathematics and a world wind atlas to produce a wind distribution map of all Jordan provinces and the most suitable sites for wind farms. It was observed that when the hub's elevation is increased from 50 to 200 meters, the mean power density increases. The highest monthly wind speed was

determined at Aqaba, the minimum at Al-Salt, and the mean power density increases toward the southern provinces.

The purpose of this work was to develop an approach for accurate wind energy evaluation in the case of three samples of Jordanian locations. The research examined average wind speed and power, Weibull distribution, density and output power, characteristic of capacity factor. In addition to statistical approaches, a mathematical model was used to determine the desired parameters. Additionally, a wind rose for each site location was drawn, including speed variation, major directions, frequency, and energy. Finally, the optimum capacity for prospective wind farm determined, and various types of wind turbines proposed.

METHODOLOGY

The location site selection

Some organizations, such as the Ministry of Energy and Mineral Potential (MEMR) and the Royal Scientific Society of Jordan built precise measurement devices to assess the wind energy resources of various Jordanian locations [23]. Most of Jordan's wind energy installations are located in the southern regions (MEMR, 2018). In the north of Jordan, there are small and ancient wind power plants in Hofa and Ibrahimiya, with an electrical capacity that does not exceed 320 kW and 1125 kW, respectively [24].

In order to comprehend wind statistics, it is worth noting the diversity of Jordan's terrain, which results in significant variances in wind flow and turbulence. Jordan's topography, which stretches from north to south, may be divided into three primary regions: (A) the Jordan valley (Ghor) region, (B) the highland and plain plateau region, and (C) the arid region (Figure 1). Three locations in southern Jordan were selected for this study to investigate the installation of wind farms: the Ma'an, Batn Al-Ghoul and Agaba areas. The Ma'an region is a desert area with huge open expanses, located 10 kilometers northwest of Ma'an city and 210 kilometers north of Amman city. The Aqaba area is a desert region with mountain ranges to the northwest of Aqaba. Batn Al-Ghoul is 65 kilometers southeast of Ma'an, around halfway between Maan and Al Mudawara. Mountains, hills, and arid regions are intermingled with scattered plants in these locations. The suggested research locations are in regions designated as a priority for the development of wind farm projects.

Data collection

The speed wind data was obtained by masts with a height of around 50 m, and recorded readings every 10 minutes. The accumulated wind speed throughout the day was recorded. Monthly wind speeds were calculated as shown in Table 1. It was observed that the Ma'an region has the highest mean wind speed during February and April, whereas the Aqaba region has the highest mean wind speed during the summer. The Batn Al-Ghoul area, on the other hand, displays winter peak wind speed. The average velocity is a crucial parameter of wind spectrum data at a location, and it is calculated using the formula:

$$\bar{\upsilon} = \frac{1}{N}\sum_{i=1}^{N} v \tag{1}$$

where: $\bar{\upsilon}$ – the average wind velocity (m/s),
v – wind speed (m/s),
N – the number of wind speed data.

When calculating wind energy, the velocity should be weighted for its power content while calculating the average. As a result, the average wind velocity is calculated as follows [25]:

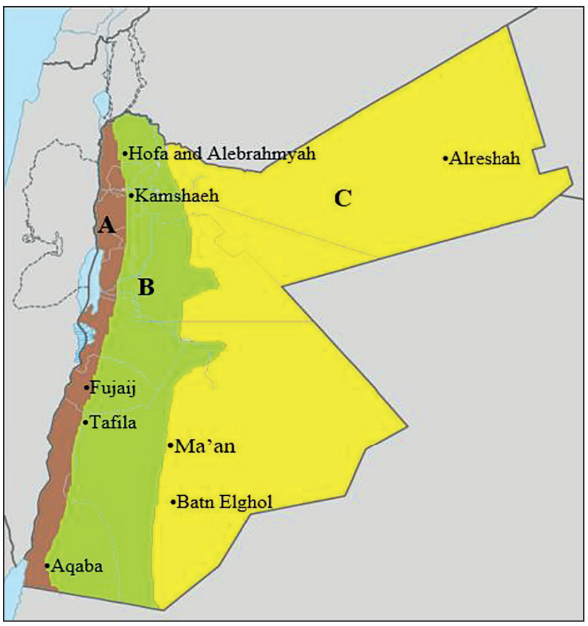

Fig. 1. The perspective wind power locations in Jordan: A – the Jordan valley (Ghor) region, B – the highland and plain plateau region, C – the arid region

Table 1. Monthly average wind speed (m/s) for selected locations

Month	Ma'an region, H = 51 m E 758451, N 3350752	Aqaba region, H = 50 m E 700245, N 3298836	Batn Al-Ghoul region, H = 50 m E 781955.1, N 3295469.9
Jan	4.17	3.69	4.15
Feb	5.42	4.15	4.54
Mar	3.65	4.85	4.72
Apr	5.04	5.14	4.68
May	3.74	5.36	4.64
Jun	4.10	5.19	3.79
July	4.25	5.20	2.97
Aug	3.93	5.28	3.00
Sep	3.41	5.43	3.35
Oct	4.01	4.82	3.63
Nov	3.42	5.14	3.61
Dec	3.87	3.96	3.65

$$\bar{\upsilon} = \left(\frac{1}{N}\sum_{i=1}^{N} v^3\right)^{1/3} \tag{2}$$

To calculate the standard deviation σ of the time-series of recorded monthly wind speed data, Eq. (3) was used [26]:

$$\sigma = \sqrt{\frac{1}{N-1}\sum_{i=1}^{N}(v - \bar{\upsilon})^2} \tag{3}$$

where: σ – standard deviation of the observed data.

Statistical analysis

Many different distributions, including Weibull, Rayleigh, gamma, lognormal, and logistic, are used to fit a recorded wind speed probability distribution in a specific location during a period of time [13]. The Weibull density function represents the probability $f(v)$ for a specific wind speed value within a specified time, and is given by Eq. (4) [27, 28]:

$$f(v) = \frac{k v^{k-1}}{c^k}\, \mathrm{e}^{-\left(\frac{v}{c}\right)^k} \tag{4}$$

where: c – the scale parameter (m/s),
v – the wind speed (m/s),
k – the shape parameter.

The cumulative Weibull distribution $F(v)$ can be determined using Eq. (5):

$$F(v) = 1 - e^{-\left(\frac{v}{c}\right)^k} \tag{5}$$

There are six different numerical approaches for estimating Weibull parameters: graphical method, maximum likelihood estimation method, energy pattern factor method, modified maximum likelihood estimation method, method of moment, and empirical method [25]. In this statistical study, three methods were chosen (EM, EPFM, and MOM) for estimating Weibull parameters: shape parameter (k), and scale parameter (c).

Empirical method

This approach is also known as the least-square method standard deviation and mean wind speed method. When the mean speed ($\bar{\upsilon}$) and standard deviation (σ) for a location are known, the Weibull shape and scale parameters can be determined using Eq. (6):

$$(\sigma \times \bar{\upsilon})^2 = \frac{\Gamma\left(\frac{2+k}{k}\right)}{\Gamma^2\left(\frac{1+k}{k}\right)} - 1 \tag{6}$$

Following the determination σ and $\bar{\upsilon}$, the Weibull parameters are calculated using Eqs. (7) and (8) [29]:

$$k = (\sigma/\bar{\upsilon})^{-1.086} \tag{7}$$

$$c = \bar{\upsilon} \,/\, \Gamma\left(1 + \frac{1}{k}\right) \tag{8}$$

where: $\Gamma(x)$ – gamma function, can be approximated by [30]:

$$\Gamma(x) = \left(\left(\sqrt{2\pi x}\right)(x^{x-1})(e^{-x})\right.$$
$$\left.\left(1 + \frac{1}{12x} + \frac{1}{288x^2} - \frac{139}{51840x^3} + \cdots\right)\right. \tag{9}$$

and

$$\Gamma\left(1 + \frac{1}{k}\right) = \frac{a_2(k)}{k}\left(1 + \frac{1}{k}\right)^{\frac{1}{k}} \tag{10}$$

where: x – any positive real number (x = 0, 1, 2, ...).

and

$$a_2(k) = -0.0053k^3 + 0.0837k^2 + 0.502k + 0.3429 \quad (11)$$

Energy pattern factor method

The EPFM approach is a simpler formulation, easier to implement, and involves less computing way of determining the possible wind power density of an area, with wind speed fluctuation accounting for the energy power density over a particular period. This method is defined by the following Eqs. (12-14) [31]:

$$E_{pf} = V^3 / \bar{\upsilon} \quad (12)$$

$$k = 1 + (3.69 / E_{pf}^2) \quad (13)$$

$$c = \bar{\upsilon} / \Gamma(1+1/k) \quad (14)$$

where: E_{pf} – the energy pattern factor.

Method of moment

The MOM approach was one of the first estimating methodologies. To calculate the Weibull parameters, Eqs. (15-16) were used:

$$k = \left[\frac{0.9874}{\frac{\sigma}{\bar{\upsilon}}}\right]^{1.0983} \quad (15)$$

$$c = \frac{v}{\Gamma(\frac{1}{k}+1)} \quad (16)$$

Wind power density estimation

Wind power density (WPD) is a key factor in determining available resources at potential sites. Wind power per unit swept area of a turbine (A) is proportional to the cube of wind speed (v) and is given by Eq. (17):

$$P(v) = 1/2\ \rho \cdot A \cdot v^3\ (\mathrm{W/m^2}) \quad (17)$$

where: ρ – the air density.

Monthly or annual wind power density per unit area of a location based on a Weibull or Rayleigh density function can be determined by Eqs. (18-19):

$$\mathrm{WPD} = P_w/A = 1/2\ \rho \cdot c^3 \cdot \Gamma(1+3/k) \quad (18)$$

$$\mathrm{WPD} = P_r/A = 3/\pi\ \rho \cdot \bar{\upsilon}^3 \quad (19)$$

where: P_w is the Weibull power density and P_r is the Rayleigh power density.

The $\Gamma(1+3/k)$ was obtained from Eq. (20) [32]:

$$\Gamma\left(1+\frac{3}{k}\right) = \frac{a_3(k)}{k}\ (1+\frac{2}{k})^{\frac{1}{k}} \quad (20)$$

where:

$$a_3(k) = -0.012k^3 + 0.1958k^2 - 0.1496k + 1.5179 \quad (12)$$

Wind energy density estimation

Wind energy density (WED) can be calculated by multiplying WDP by the number of hours (T). To obtain the yearly WED, multiply by 8760 h to obtain the wind energy density in kWh/m^2 on a Weibull or Rayleigh density function, as provided by Eqs. (22-23):

$$\mathrm{WED} = 1/2\ \rho\ c^3\ \Gamma(1+3/k)\ T \quad (22)$$

$$\mathrm{WED} = 3/\pi\ \rho\ \bar{\upsilon}^3\ T \quad (23)$$

It should be mentioned that two criteria are required for the development of a wind energy project: (i) the most probable wind speed, and (ii) the speed carrying the maximum energy to the wind regime. According to the wind's cubic velocity-power relationship, the velocity supplying the maximum energy is usually higher than the most frequent wind velocity [33]. The following equation can be used to compute the most probable wind speed (U_{Fmax}) using the Weibull parameters [34]:

$$U_{Fmax} = c \cdot [(k-1)/k]^{1/k} \quad (24)$$

The speed carrying the maximum energy (U_{Emax}) is obtained by the following equation:

$$U_{Emax} = c \cdot [(k+2)/k]^{1/k} \quad (25)$$

Wind rose evaluation

The directional frequency distribution is a key property of wind resources. A wind rose is a polar plot that shows the frequency of occurrence by direction. A wind rose can also assess speed or energy distribution. Some plots frequently indicate the time the wind flowed in specific speed ranges by splitting each map segment into separate color bands. Another figure shows the fraction of total energy in the wind that comes from each direction. These plots are occasionally blended into one. The plots are generated by sorting the wind data into the necessary number of sectors, which is usually 12 or 16, and then computing the relevant statistics for each sector.

Several ways to design wind rose include utilizing specific websites, special wind analysis applications, or Microsoft Excel. The following are the procedures for plotting a wind rose in a Microsoft Excel program: (i) arrange the wind data in a table based on the direction and speed

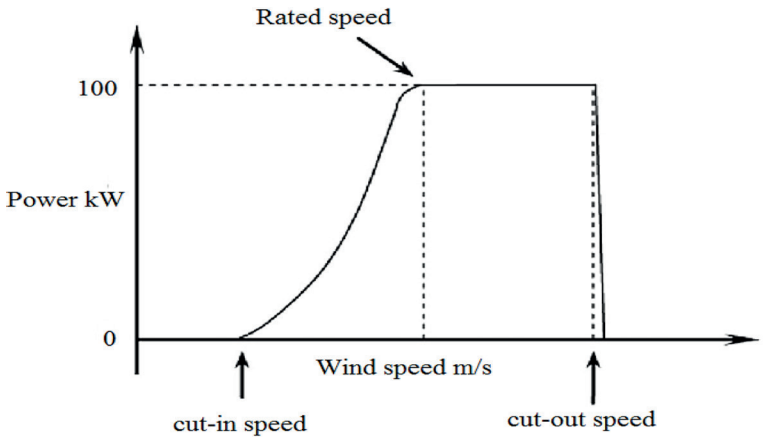

Fig. 2. The ideal wind turbine power curve

classifications; (ii) determine the number of observations for each wind speed class and direction; (iii) create a wind rose data highlight table and place a filled radar with markers chart; (iv) the percentage of time the wind blows from any direction is calculated by dividing the frequency of an observed data value by the total data number values and then calculating the percent style; (v) wind energy is estimated by taking the product of the percentage frequency and the cube of the mean wind for each direction and dividing it by the sum of those products for all directions.

Power and energy output

The most significant metric for assessing a wind turbine is its annual energy output. The ideal wind turbine power curve is depicted in Figure 2, in which the turbine starts to operate at the cut-in speed (V_c), then the power output rises with wind speed, following a cubic curve until wind speed reaches the rated speed (V_r), at which point the turbine begins to operate at its rated power. When the wind speed exceeds the cut-out speed, the rotor comes to a cut-out speed (V_o). The power of a wind turbine lies between its cut-in speed and its rated speed, for the speed range $V_c \leq V \leq V_r$ can be stated as Eq. 26 [35]:

$$P = P_R \left(\frac{V^2 - V_c^2}{V_r^2 - V_c^2}\right) \tag{26}$$

where: P – wind turbine power at speed V;
$P = P_R$ for $V_c \leq V \leq V_o$, P = 0 for $V \leq V_c$ and $V \geq V_o$.

The capacity factor (C_F) is one of the wind turbine performance metrics that must be addressed. The capacity factor of a wind turbine is equal to the actual energy output (E_T) for the year divided by the energy output if the turbine operated at its rated power output (P_R) for the year (T) [21]:

$$C_F = \frac{E_T}{T\,P_R} \tag{27}$$

The energy generated by any wind turbine at any site over a year may be calculated by multiplying C_F by the rated power and time period. The yearly energy production is the primary criterion for assessing a wind turbine; one technique for estimating annual energy output is to utilize the wind power density method, as shown below in Eq. 28 [36]:

$$E_T = C_F \cdot P_R \cdot h \tag{28}$$

$$P_R = A \cdot \text{WPD} \tag{29}$$

where: h – number of hours in a year (8760).

RESULTS

The Weibull parameters results

The shape parameter (k) controls the distribution's width; a higher value suggests a smaller frequency distribution (i.e., a steadier, less variable wind). The scale parameter (c) has a speed dimension closely tied to the mean wind speed. The results of k and c parameters presented in Table 2 were derived using Eqs. (7-8, 13-16) for wind speed data obtained of a selected areas in South of Jordan. The results show that the average values of k was from 1.5 for the Ma'an region, to 2.2 for the Aqaba region. Average c values ranges from 4.3 to 6.8.

Figure 3a depicts the EPFM approach of shape parameter, which reflects the range of wind speed distributions; greater values of k suggest

Table 2. The values of Weibull parameters according to three approaches: MOM, EM, and EPFM

Month	Ma'an region						Aqaba region						Batn Al-Ghoul region					
	MOM		EM		EPFM		MOM		EM		EPFM		MOM		EM		EPFM	
	k	c	k	c	k	c	k	c	k	c	k	c	k	c	k	c	k	c
Jan	1.8	4.7	1.8	5.8	1.9	4.7	2.0	4.2	2.1	5.2	2.1	4.2	1.9	4.7	1.9	5.8	2.2	4.7
Feb	1.8	6.1	1.8	7.5	1.9	6.1	2.1	4.7	2.1	5.9	2.2	4.7	1.9	5.1	1.9	6.4	2.2	5.1
Mar	1.1	3.8	1.1	4.0	1.2	3.8	2.1	5.5	2.2	6.9	2.2	5.5	1.8	5.3	1.9	6.6	1.9	5.3
Apr	1.8	5.7	1.8	7.0	1.9	5.7	2.1	5.8	2.1	7.3	2.2	5.8	1.9	5.3	1.9	6.5	1.9	5.3
May	1.1	3.9	1.1	4.1	1.2	3.8	2.2	6.1	2.2	7.7	2.2	6.1	1.8	5.2	1.9	6.5	1.9	5.2
Jun	1.1	4.2	1.1	4.4	1.2	4.3	2.1	5.9	2.1	7.4	2.2	5.9	1.5	4.2	1.5	5.0	1.3	4.1
July	1.1	4.4	1.1	4.6	1.2	4.5	2.1	5.9	2.2	7.4	2.2	5.9	1.1	3.1	1.1	3.3	1.2	3.1
Aug	1.1	4.0	1.1	4.3	1.2	4.1	2.1	6.0	2.2	7.5	2.2	6.0	1.1	3.1	1.1	3.3	1.2	3.2
Sep	1.1	3.5	1.1	3.7	1.2	3.6	1.1	6.1	2.1	7.7	2.2	6.1	1.2	3.6	1.2	4.0	1.3	3.6
Oct	1.8	4.5	1.8	5.6	1.9	4.5	2.1	5.4	2.1	6.9	2.2	5.4	1.8	4.1	1.8	5.1	1.9	4.1
Nov	1.9	3.8	1.9	4.8	2.0	3.9	2.1	5.8	2.1	5.9	2.2	5.8	1.9	4.1	1.9	5.1	2.0	4.1
Dec	1.8	4.3	1.8	5.4	1.9	4.9	2.1	4.5	2.1	5.6	2.2	4.5	1.8	4.1	1.8	5.1	1.9	4.1
Average	1.5	4.4	1.5	5.1	1.5	4.5	2.0	5.5	2.1	6.8	2.2	5.5	1.6	4.3	1.7	5.2	1.7	4.3

the most probable wind speeds while remaining within the tight ranges [37]. The maximum value of *k* was from Aqaba location, while the lowest value was from the Ma'an area, indicating that winds have a wide range of speeds. In turn, Figure 3b displays the scale parameters from the EPFM approach, which reflects an increase the wind energy potential by increasing the value of *c* [25]. For the Ma'an area, the average values of *c* were from 4.4 to 5.1 m/s, with the maximum value reaching 7.5 m/s in February and the minimum reaching 3.5 m/s in September. For the Aqaba and Batn Al-Ghoul locations, the MOM and EPFM values of *c* were 5.5 m/s and 4.3 m/s, respectively, while the EM displays the highest values in Aqaba at 6.6 m/s and Batn Al-Ghoul at 5.2 m/s. The lowest value of *c* was 3.1 m/s in the Batn Al-Ghoul region in July and August, while the maximum value was 7.7 m/s in the Aqaba region in May and September. Data shows that the Aqaba area location has a large wind power potential since the value of scale parameter was the highest.

Table 3 depicts the annual fluctuation of the EPFM's mean wind speed parameters ($\bar{\upsilon}$, σ, U_{Fmax}, U_{Emax}) as well as WPD and WED in several Jordanian southern regions. The highest average speed in the Aqaba location was 4.9 m/s, with the peak wind speed occurring from April to November at 5.1 m/s. The best values of average wind speed in the Ma'an location were from January to July, whereas the best values of average wind speed in Batn Al-Ghoul were from January to May. Furthermore, Table 3 indicates the most probable wind speed carrying the maximum energy, with the highest

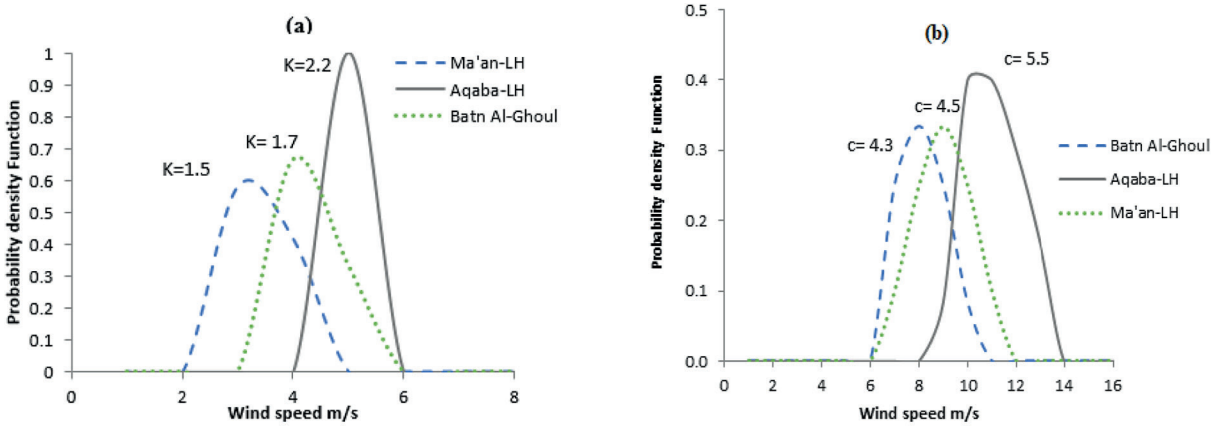

Fig. 3. Weibull probability density function for shape parameter (a), and scale parameter (b)

Table 3. The typical characteristic and mean wind speed in selected locations

M: Ma'an, A: Aqaba, B: Batn Al-Ghoul																		
Month	M	A	B	M	A	B	M	A	B	M	A	B	M	A	B	M	A	B
	ū (m/s)			σ			WPD (W/m^2)			WED (kWh/m^2)			U_{Fmax} (m/s)			U_{Emax} (m/s)		
Jan	4.2	3.7	4.2	2.4	1.9	2.3	87.5	55.4	76.6	65.1	41.2	57.0	3.2	3.1	3.5	4.2	3.7	4.2
Feb	5.4	4.2	4.5	3.1	2.0	2.5	194.8	76.0	99.2	144.9	56.6	73.8	4.1	3.6	3.9	8.9	6.3	6.9
Mar	3.6	4.9	4.7	3.3	2.4	2.7	124.1	120.5	128.4	92.3	89.6	95.5	0.7	4.2	3.6	3.6	4.9	4.7
Aprl	5.0	5.1	4.7	2.9	2.6	2.6	155.7	144.9	123.2	115.8	107.8	91.7	3.8	4.4	3.6	5.0	5.1	4.7
May	3.7	5.4	4.6	3.4	2.6	2.6	132.9	162.0	121.6	98.9	120.5	90.5	0.8	4.6	3.6	3.7	5.4	4.6
Jun	4.1	5.2	3.8	3.8	2.6	2.6	177.0	148.2	115.3	131.7	110.3	85.8	0.8	4.5	1.3	4.1	5.2	3.8
July	4.2	5.2	3.0	3.9	2.6	2.7	197.1	148.7	67.1	146.6	110.6	49.9	0.8	4.5	0.6	4.2	5.2	3.0
Aug	3.9	5.3	3.0	3.6	2.6	2.8	154.4	155.6	69.5	114.9	115.8	51.7	0.8	4.6	0.6	3.9	5.3	3.0
Sep	3.4	5.4	3.4	3.1	2.7	2.8	100.9	169.6	75.7	75.0	126.2	56.3	0.7	4.7	1.3	3.4	5.4	3.4
Oct	4.0	4.8	3.6	2.3	2.4	2.1	77.9	119.0	59.9	58.0	88.5	44.5	3.1	4.1	2.7	4.0	4.8	3.6
Nov	3.4	5.1	3.6	1.9	2.1	2.0	47.5	97.8	54.7	35.3	72.8	40.7	2.7	5.3	2.9	3.4	5.1	3.6
Dec	3.9	4.0	3.7	2.3	2.0	2.1	72.4	66.7	59.8	53.9	49.6	44.5	2.9	3.4	2.8	3.9	4.0	3.7
Average	4.1	4.9	3.9	3.0	2.4	2.5	126.8	122.0	87.6	94.4	90.8	65.2	2.0	4.2	2.5	4.1	4.9	3.9

average value in the Aqaba area being 4.2 m/s and the lowest average value in the Ma'an location being 2.0 m/s. The lowest monthly most probable wind speed carrying the maximum energy value was achieved in August in the Batn Al-Ghoul location (0.6 m/s), while the highest value was found in November in the Aqaba location (5.3 m/s). The highest value of the wind speed carrying the maximum energy occurs in the Ma'an area at 8.9 m/s recorded in February, and the lowest value of 3.0 m/s obtained in the Batn Al-Ghoul area in July and August. Additionally, Table 3 reveals that the largest average values of WPD in the Ma'an and Aqaba locations were greater than 120 W/m^2. In turn, the lowest wind potential densities were achieved in the Batn Al-Ghoul area, where WPD was 87.6 W/m^2. For the selected locations: Ma'an, Aqaba, and Batn Al-Ghoul, the maximum monthly WPD values were reported from February to September, March to October, and March to June, respectively. Finally, Table 3 compared the wind energy densities in the Aqaba, Ma'an, and Batn Al-Ghoul areas. It demonstrates that WED average value in the Ma'an area is higher than in the Aqaba and Batn Al-Ghoul areas. The maximum values of WED were recorded in February and July in the Ma'an region at over 140 kWh/m^2, in May and September in the Aqaba region at about 120 kWh/m^2, and from March to June in the Batn Al-Ghoul region of above 85 kWh/m^2.

Wind rose results

The wind rose illustrates the temporal distribution of wind blows as well as the azimuthal distribution of wind speed from a certain direction. Estimating suitable wind direction is critical, since the quantity of wind energy captured by horizontal axis wind turbine, which are often utilized for energy production, depends on the direction in which these turbines are situated. As a result, the turbine must be positioned with the rotor pointing in the best wind direction.

Figure 4 demonstrates the (a) mean wind speed rose in the 2–10 m/s range, (b) direction, (c) frequency, and (d) energy in the Ma'an, Aqaba, and Batn Al-Ghoul locations. The maximum wind gusts registered for the Ma'an area were above 8 m/s for daily data recorded (Fig. 4a). The main wind direction is toward the West, West-Southwest, and West-Northwest, which can be explained as a wind from the west that is slightly angled to the south and north but is more confirmed on the west, as shown in the direction rose distribution (Fig. 4b). The frequency rose, which indicates the percentage of time that receives wind from a certain direction, clearly shows that about 25% of the time the wind blows, it varies between the North and the East, as shown in Figure 4c. Finally, the energy rose is the product of the time and the cube of the wind velocity, which may be used to identify the energy available from various directions. As indicated in Figure 4d, energy-rich winds blow from the West-Southwest

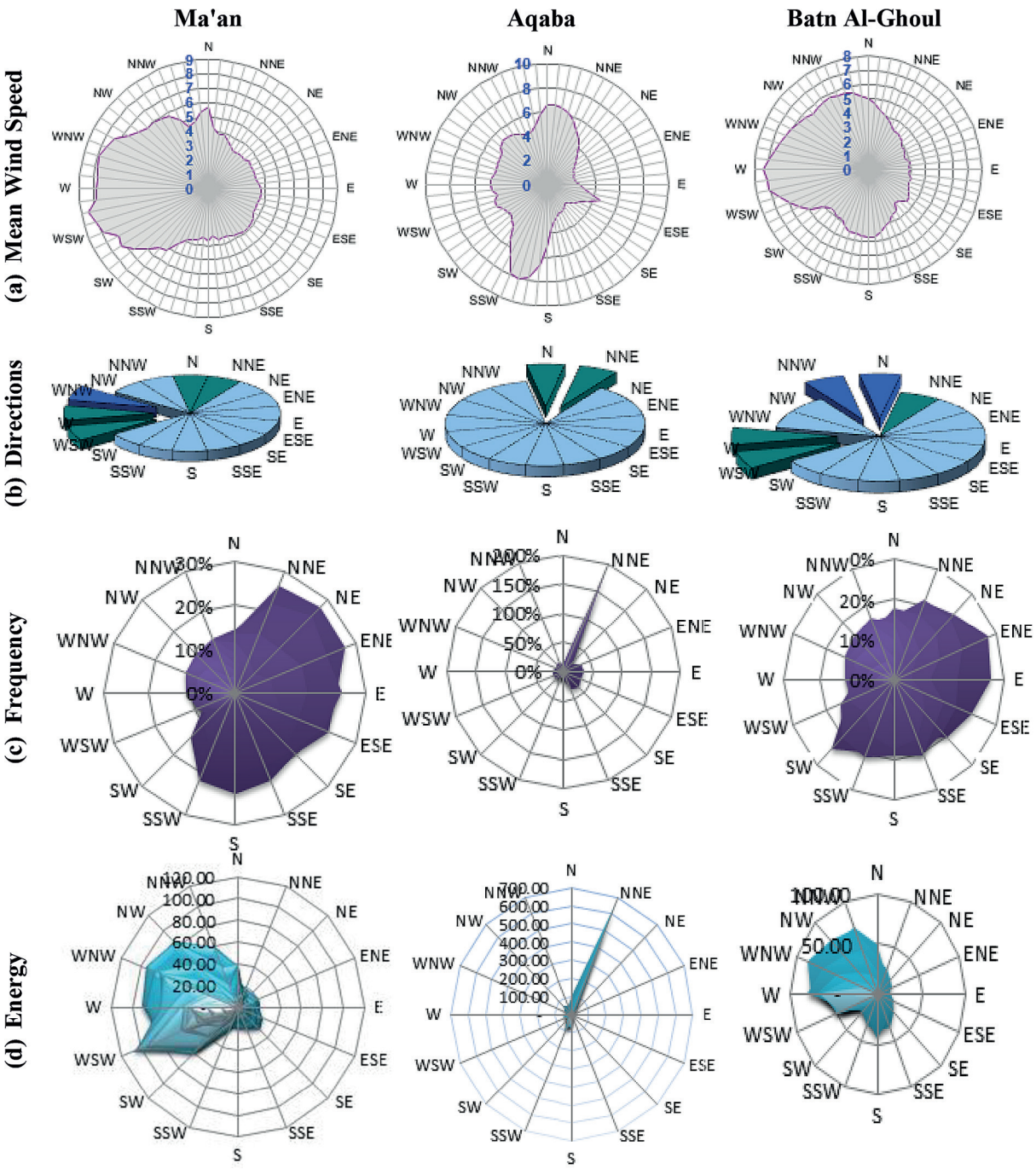

Fig. 4. Wind rose schematic diagram of wind speed variation, main directions, frequency, and energy for the Ma'an, Aqaba, and Batn Al-Ghoul areas

Table 4. Technical data of wind turbines

Parameter	Wind turbine type		
	Gamesa-G114	Gamesa-G132	Vestas-V136
Power output (kW)	2000	3300	3450
Cut-in speed (m/s)	3.5	2	3
Cut-out speed (m/s)	25	25	22.5
Rated speed (m/s)	10	10	11
Hub height (m)	93/120/140	84/97/114/134	82 /112 /132
Rotar diameter (m)	114	132	136
Swept area (m^2)	10207	13685	14257

Table 5. Estimated annual energy output depending of wind turbine type

Area	Energy output for one year (GW·h)		
	Gamesa-G114	Gamesa-G132	Vestas-V136
Ma'an	4.20	5.87	6.31
Aqaba	4.99	6.92	7.36
Batn Al-Ghoul	2.97	3.64	4.29

in the Ma'an region. For the Aqaba location, the wind velocity and average strength of the wind spectrum exceed 6 m/s for daily data recorded, with the most common wind directions being North and North-Northeast. The frequency rose exhibited a significant proportion compared to other studied sites, reaching above 200%. The most energy-rich winds come from the north-northeast, and a lot of energy is available. In the Batn Al-Ghoul region, the average strength of the wind spectrum is greater than 7 m/s for daily data recorded, and the major wind direction is toward the North and North-Northwest, with the strongest toward the West and West-Southwest. Compared to other analyzed locations, the frequency rose has a low proportion. Most available energy comes from the West and the Northwest and is considered low.

Energy output results

Table 4 shows the technical data of wind turbine examples [38]. It was used to estimate the yearly energy output for selected area locations, as displayed in Table 5. It was shown, that the Aqaba area definitely has the highest wind energy potential. Furthermore, as the rated power increased, then energy production increased as well.

CONCLUSIONS

On the basis of the investigation results obtained, the following conclusions can be drawn. To estimate wind power density and predicting wind potential the energy pattern factor method was confirmed to be the best of the all others. The highest wind speed in the Aqaba area noted from April to November was in range of 5.1–5.4 m/s. The Aqaba area has the greatest wind energy potential and the highest wind energy density. At other hand, the worst wind energy density was noted at the Batn Al-Ghoul area. The highest average values of speed carrying the maximum energy were noted in the Aqaba area as well. For the Aqaba area, the most common wind directions were North and North-Northeast, so a lot of energy is available compared to other studied sites. Estimated annual energy output, depending of wind turbine type, was obtained in the range of 4.99–7.36 GWh.

Acknowledgements

This article was supported by the Lublin University of Technology (Grant No. FD-20/IS-6/002).

REFERENCES

1. Al-Amayreh M.I., Alahmer A., Manasrah A. A novel parabolic solar dish design for a hybrid solar lighting-thermal applications. Energy Reports 2020; 6: 1136–43.
2. Khaled M.B., Qandil A., Abdallatif N., Beithou N., Alsaqoor S., Alahmer A, et al. Heating and Cooling Device for Motorhomes and Caravans. Int J Thermofluids 2022: 100193.
3. David B.R., Spencer S., Miller J., Almahmoud S., Jouhara H. Comparative environmental life cycle assessment of conventional energy storage system and innovative thermal energy storage system. Int J Thermofluids 2021; 12: 100116.
4. Al-Manea A., Al-Rbaihat R., Kadhim H.T., Alahmer A., Yusaf T., Egab K. Experimental and Numerical Study to Develop TRANSYS Model for an Active Flat Plate Solar Collector with an Internally Serpentine Tube Receiver. Int J Thermofluids 2022: 100189.
5. Alkhalidi A., Alqarra K., Abdelkareem M.A., Olabi A.G. Renewable Energy Curtailment practices in Jordan and Proposed Solutions. Int J Thermofluids 2022: 100196.
6. NEPCO company. Annual reports 2019. http://www.nepco.com.jo/store/docs/web/2019_en.pdf.
7. Alahmer A., Ajib S. Solar cooling technologies: State of art and perspectives. Energy Convers Manag 2020; 214: 112896.
8. Brower M. Wind resource assessment: a practical guide to developing a wind project. John Wiley & Sons; 2012.
9. Corke T., Nelson R. Wind energy design. CRC

Press; 2018.

10. Iyinomen D.O. Numerical and experimental analyses of ablation measurements in expansion wind tunnel facilities using a new plasma pre-heating technique. Int J Thermofluids 2020; 3: 100019.
11. Chang T.P. Performance comparison of six numerical methods in estimating Weibull parameters for wind energy application. Appl Energy 2011; 88: 272–82.
12. Ouahabi M.H., Elkhachine H., Benabdelouahab F., Khamlichi A. Comparative study of five different methods of adjustment by the Weibull model to determine the most accurate method of analyzing annual variations of wind energy in Tetouan-Morocco. Procedia Manuf 2020; 46: 698–707.
13. Azad A.K., Rasul M.G., Yusaf T. Statistical diagnosis of the best Weibull methods for wind power assessment for agricultural applications. Energies 2014; 7: 3056–85.
14. Ramachandra T.V., Subramanian D.K., Joshi N.V. Wind energy potential assessment in Uttara Kannada district of Karnataka, India. Renew Energy 1997; 10: 585–611.
15. Bassyouni M., Gutub S.A., Javaid U., Awais M., Rehman S., Hamid S.A., et al. Assessment and analysis of wind power resource using weibull parameters. Energy Explor Exploit 2015; 33: 105–22.
16. Aukitino T., Khan M.G.M., Ahmed M.R. Wind energy resource assessment for Kiribati with a comparison of different methods of determining Weibull parameters. Energy Convers Manag 2017; 151: 641–60.
17. Kidmo D.K., Danwe R., Doka S.Y., Djongyang N. Statistical analysis of wind speed distribution based on sixWeibull Methods for wind power evaluation in Garoua, Cameroon. J Renew Energies 2015; 18: 105–25.
18. Marashli A., Alburdaini M., Al-Rawashdeh H., Shalby M. Statistical Analysis of Wind Speed Distribution Based on Five Weibull Methods for Wind Power Evaluation in Maan, Jordan. J Energy Technol Policy 2021; 11: 55–70. https://doi.org/10.7176/JETP/11-4-05.
19. Alsaad M.A. Wind energy potential in selected areas in Jordan. Energy Convers Manag 2013; 65: 704–8.
20. Bataineh K.M., Dalalah D. Assessment of wind energy potential for selected areas in Jordan. Renew Energy 2013; 59: 75–81.
21. Ammari H.D., Al-Rwashdeh S.S., Al-Najideen M.I. Evaluation of wind energy potential and electricity generation at five locations in Jordan. Sustain Cities Soc 2015; 15: 135–143.
22. Alrwashdeh S.S. Map of Jordan governorates wind distribution and mean power density. Int J Eng Technol 2018; 7: 1495–500.
23. Davies M., Hodge B., Shakeeb A., Wang Y. Developing renewable energy projects-A guide to achieving success in the Middle East/Eversheds, PwC 2016.
24. Al-omary M., Kaltschmitt M., Becker C. Electricity system in Jordan: Status & prospects. Renew Sustain Energy Rev 2018; 81: 2398–409.
25. Sathyajith M. Wind energy: fundamentals, resource analysis and economics. Springer Science & Business Media; 2006.
26. Celik A.N. A statistical analysis of wind power density based on the Weibull and Rayleigh models at the southern region of Turkey. Renew Energy 2004; 29: 593–604.
27. Kang D., Ko K., Huh J. Comparative study of different methods for estimating Weibull parameters: a case study on Jeju Island, South Korea. Energies 2018; 11: 356.
28. Gungor A., Gokcek M., Uçar H., Arabacı E., Akyüz A. Analysis of wind energy potential and Weibull parameter estimation methods: a case study from Turkey. Int J Environ Sci Technol 2020; 17: 1011–20.
29. Mohsin A., Zhang K., Hu J., Tariq M., Zaman W.Q., Khan I.M., et al. Optimized biosynthesis of xanthan via effective valorization of orange peels using response surface methodology: A kinetic model approach. Carbohydr Polym 2018; 181: 793–800.
30. Jamil M., Parsa S., Majidi M. Wind power statistics and an evaluation of wind energy density. Renew Energy 1995; 6: 623–8.
31. Akdağ S.A., Güler Ö. A novel energy pattern factor method for wind speed distribution parameter estimation. Energy Convers Manag 2015; 106: 1124–33.
32. Touré S. Investigations into some simple expressions of the gamma function in wind power theoretical estimate by the Weibull distribution. J Appl Math Phys 2019; 7: 2990–3002.
33. Afungchui D., Aban C.E. Analysis of wind regimes for energy estimation in Bamenda, of the North West Region of Cameroon, based on the Weibull distribution. J Renew Energies 2014; 17: 137–47.
34. Adaramola M.S., Agelin-Chaab M., Paul S.S. Assessment of wind power generation along the coast of Ghana. Energy Convers Manag 2014; 77: 61–9.
35. Pallabazzer R. Evaluation of wind-generator potentiality. Sol Energy 1995; 55: 49–59.
36. Clark N. Small wind: planning and building successful installations. Academic Press; 2013.
37. Manwell J.F., McGowan J.G., Rogers A.L. Wind energy explained: theory, design and application. John Wiley & Sons; 2010.
38. Matysik L.B. Wind turbine models 2021. https://en.wind-turbine-models.com/turbines/1336-gamesa-g132-3.3mw (Accessed October 30, 2021).